

Development of Wide-Band Geometry Dependent RF Planar Spiral Inductor SPICE Model

Elissaveta D. Gadjeva, Marin H. Hristov, and Vladislav P. Durev

Abstract—Parameterized wide-band geometry dependent SPICE models for on-chip planar spiral inductors are developed in the paper. Model descriptions are presented in the form of PSpice model and in schematic view. The models are realized in the Cadence Capture and Cadence PSpice environment. The developed computer models can be used for adequate computer modeling and simulation of RF circuits. The geometry dependence of the model parameters allows geometry optimization and design automation of spiral inductors. The simulation results are compared to the measurement data for the model verification demonstrating the validity of the computer models.

Index Terms—Compter models, Planar spiral inductors, PSpice simulation, Scalable models, Q factor

I. INTRODUCTION

THE development of radio-frequency integrated circuits requires adequate and effective tools for modeling and simulation. The on-chip planar inductor is critical component in implementing RF circuits. Many papers are published in the recent years, devoted on accurate modeling, model parameter extraction and optimization of on-chip spiral inductors.

The physical model of planar spiral inductor on silicon (π -model) shown in Fig. 1 [1] is a very popular model used in microelectronic design. Its model parameter values can be expressed directly using the geometry of the spiral inductor. The skin effect at high frequencies is modeled using a frequency dependent series resistance. Several extraction procedures are developed for the physical spiral inductor model – direct procedures [2], optimization based procedures [3]. A number of approaches to geometry optimization of spiral inductors are proposed based on optimization using geometric programming [4], genetic algorithms, etc. An approach is developed in [5] to direct parameter extraction based on the measured S -parameters.

A modification of the π -model with frequency independent parameters is presented in Fig. 2. The two- π model taking into account the decreasing in the series resistance at higher frequencies, is shown in Fig. 3 [6]. A scalable modeling and comparison is performed in [7] for spiral inductors using enhanced π and two- π topologies with respect to the complexity of equivalent circuit models, scalable rules and the accuracy of scalable models.

The wide-band spiral inductor model, proposed in [8], is shown in Fig. 4. It is simple and has an excellent accuracy

compared to the measured results. The advantages of this model compared to the models with geometry dependent parameters consist in the frequency independence of the model parameters and in prediction the drop-down characteristics in the series resistance at higher frequencies. Several modifications of the model are proposed in [9,10]. The application of the simple parameter extraction method [11] and the systematic model parameter extraction approach [12] lead to very accurate results.

The substrate-coupled model [13] includes a substrate network to model the eddy current as shown in Fig. 5. The advantages of this model are the prediction the drop-down characteristic in the series resistance at higher frequencies compared to the π model. An enhancement of the model [13] is the scalable substrate-coupled model [14] where the parameters of the model elements are expressed as monomial expressions in terms of physical geometry.

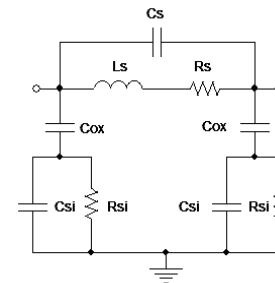


Fig. 1. Physical π - model of planar spiral inductor on silicon

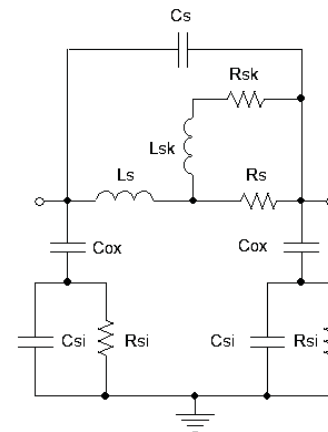


Fig. 2. Physical π - model of planar spiral inductor on silicon with frequency independent parameters

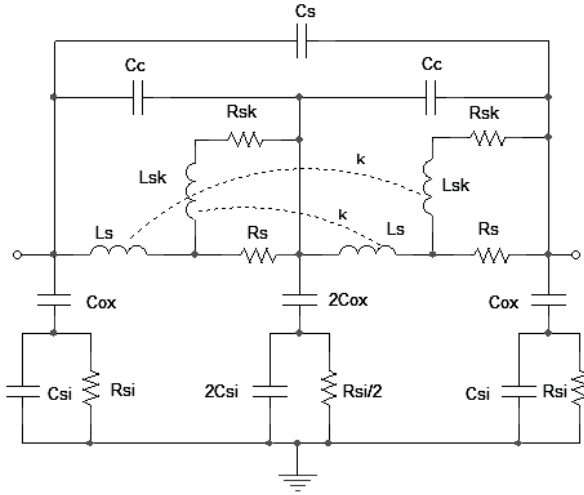
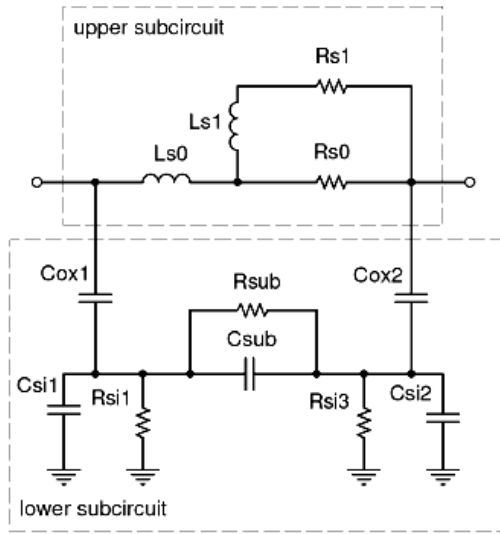
Fig. 3. Two- π model of planar spiral inductor on silicon

Fig. 4. Wide-band spiral inductor model

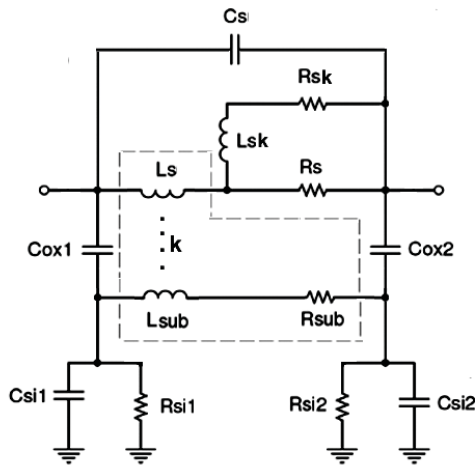


Fig. 5. Scalable substrate-coupled spiral inductor model

As a result, the model in [14] combines the advantages of the π -model and the wide-band model: geometry dependence of the model parameters and high accuracy in the whole frequency range.

In the present paper, parameterized geometry dependent computer models of planar spiral inductor are developed corresponding to the equivalent circuit in Fig. 5. They can be implemented in the general-purpose circuit simulators such as Cadence PSpice [15]. Computer models of the spiral inductor are developed using hierarchical blocks in two variants – in schematic view and based on subcircuit description using PSpice model.

II. MODEL DESCRIPTION

The model parameters of the substrate-coupled model [13] (Fig. 5) are described in Table I.

TABLE I
DESCRIPTION OF THE MODEL PARAMETERS OF THE SUBSTRATE-COUPLED MODEL

Parameter	Description
R_s, R_{sk}	wiring resistances taking into account the skin and proximity effects
L_s, L_{sk}	inductances, modeling wiring inductance of the spiral
C_{ox1}, C_{ox2}	capacitance between the spiral and the substrate
R_{si1}, R_{si2}	resistance of the substrate
C_{si1}, C_{si2}	capacitance of the substrate
C_s	parallel-plate capacitance between the spiral and the center-tap underpass
L_{sub}	represents the eddy current flowing in the substrate
R_{sub}	substrate resistance
k	coupling coefficient between L_s and L_{sub}

The equations describing the parameters of the inductor model in Fig. 5 are in the form [14]:

$$L_s = \beta_1 D_{out}^{\alpha_1} w^{b_1} s^{c_1} n^{d_1} D_{avg}^{\epsilon_1}, \quad (1)$$

$$C_s = K_d n \cdot w^2, \quad (2)$$

$$R_s = \frac{K_b l}{w}, \quad (3)$$

$$C_{ox1} = C_{ox2} = K_c l w, \quad (4)$$

$$R_{si1} = R_{si2} = \frac{K_d}{l w}, \quad (5)$$

$$C_{si1} = C_{si2} = K_e l w, \quad (6)$$

$$L_{sub} = \beta_2 D_{out}^{\alpha_2} w^{b_2} s^{c_2} n^{d_2} L_s^{\epsilon_2}, \quad (7)$$

$$R_{sub} = \beta_3 n^{\alpha_3} (w + s)^{b_3} l^{\epsilon_3} \quad (8)$$

$$k = 1 - e^{-\beta_4 n^{\alpha_4} D_{out}^{b_4} w^{c_4} s^{d_4}} \quad (9)$$

$$D_{in} = D_{out} - 2(n(s + w) - s) \quad (10)$$

$$D_{avg} = 0.5(D_{in} + D_{out}), \quad (11)$$

where the independent geometry parameters are the trace width w , the spacing between traces s , the number of turns n and the outer diameter D_{out} (Fig. 6). The dependent geometry parameters are the inner diameter D_{in} , the average diameter D_{avg} and the trace length l .

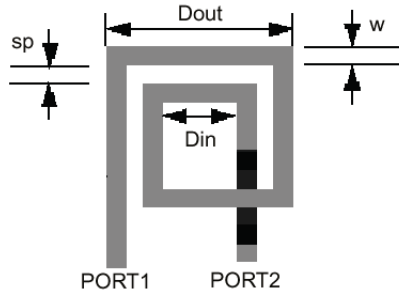


Fig. 6. Basic geometry parameters of the spiral inductor

The coefficients in the expressions (1-9) for 0.35 μm process are [14]:

$$\begin{aligned} a_1 &= 1.84, a_2 = 0.94, a_3 = 1.36, a_4 = 0.91, b_1 = -0.76, \\ b_2 &= 4.13, b_3 = 0.93, b_4 = -1.96, c_1 = -0.14, \\ c_2 &= -1.06, c_3 = -1.4, c_4 = -0.83, d_1 = 1.1, d_2 = -1.9, \\ d_4 &= 0.56, e_2 = 1.35, \beta_1 = 2.5 \times 10^{-4}, \beta_2 = 6.18 \times 10^{-7}, \\ \beta_3 &= 156, \beta_4 = -4.85 \times 10^4, K_a = 0.0415, K_b = 0.0302, \\ K_c &= 4.28 \times 10^{-3}, K_d = 8.04 \times 10^6, K_e = 2.1 \times 10^{-4} \end{aligned} \quad (12)$$

These coefficients are obtained using optimization procedure based on least-square fitting method [14], where the elements R_{sk} and L_{sk} are absorbed into R_s and L_s for practical implementation reasons. The coefficients (12) correspond to the data-fitted monomial expressions for CMOS 0.35 μm process. The coefficients for SOI 0.15 μm process are obtained in [14].

III. DEVELOPMENT OF THE COMPUTER MODEL OF SPIRAL INDUCTOR

A. Computer model in the form of hierarchical block in schematic view

The representation of the scalable substrate-coupled spiral inductor model defined as a block in *Cadence Capture* is shown in Fig. 7a. The equivalent circuit in schematic view is presented in Fig. 7b. The coefficients (12) are defines as block attributes as shown in Fig. 8a. The independent geometry parameters D_{out} , w , s and n are defined as block attributes, as shown in Fig. 8b, where the spacing between traces s is denoted by sp in the computer model. The expressions for the dependent geometry parameters D_{in} , D_{avg} and l are introduced in the value field for the corresponding block attribute (Fig. 8b). The calculated geometry parameters and the coefficients are transferred to the parameterized subcircuit at the lower hierarchical level (Fig. 7b). The parameter values of the elements are obtained using the expressions (1-9), defined in the value field of the elements as shown in Table II.

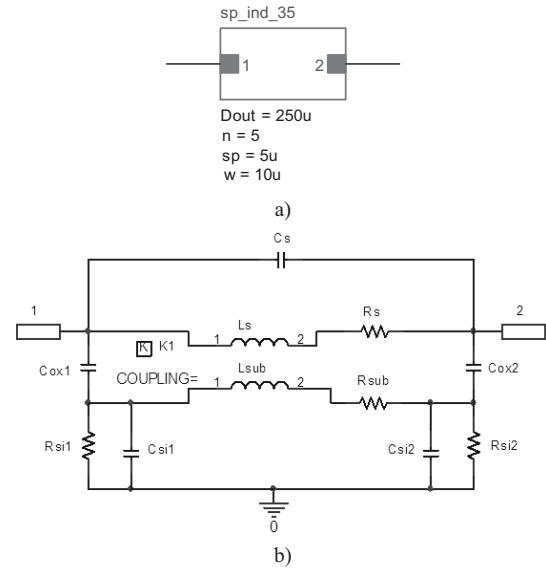


Fig. 7. Scalable substrate-coupled spiral inductor model defined as a block in *Cadence Capture*

a1	1.84	Davg	{0.5*{@Din+@Dout}}
a2	0.94	Din	{@Dout-2*{@n*{@sp+@w}-@sp}}
a3	1.36	Dout	250u
a4	0.91	L	{4*{@Davg*{@n}}
b1	-0.76	n	5
b2	4.13	sp	5u
b3	0.93	w	10u

Fig. 8. Block attributes

B. Computer model defined as a subcircuit

In order to create the computer inductor model in the form of subcircuit in accordance to the input language of the *PSpice* simulator, the block in Fig. 7a is connected to the *PSpice* model using the block attribute *PSpiceTemplate*:

```
X^@REFDES %1 %2 sp_ind_035
+ PARAMS: Dout={@Dout}, n={@n}, w={@w}, sp={@sp}
```

As a result, the subcircuit *sp_ind_035* is connected to the ports 1 and 2 and the independent geometry parameters, defined by the user, are transferred to the subcircuit. The parameters D_{out} , n , sp and w are defined as block attributes.

TABLE II
DETERMINATION OF THE MODEL PARAMETER VALUES

Parameter	Expression
R_{sub}	{@beta3*pwr(@n,@a3)*pwr((@w+@sp)*1e6,@b3)*pwr(@L*1e6,@c3)}
L_s	{@beta1*pwr(@Dout*1e6,@a1)*pwr(@w*1e6,@b1)*pwr(@sp*1e6,@c1)*pwr(@n,@d1)*1e-9}
L_{sub}	{@beta2*pwr(@Dout*1e6,@a2)*pwr(@w*1e6,@b2)*pwr(@sp*1e6,@c2)*pwr(@n,@d2)*pwr(@beta1*pwr(@Dout*1e6,@a1)*pwr(@w*1e6,@b1)*pwr(@sp*1e6,@c1)*pwr(@n,@d1),@e2)*1e-9}
k	{1-exp(@beta4*pwr(@n,@a4)*pwr(@Dout*1e6,@b4)*pwr(@w*1e6,@c4)*pwr(@sp*1e6,@d4))}
R_s	{@Kb*@L/@w}
C_s	{@Ka*@n*@w*@w}
C_{ox}	{@Kc*@L*@w}
R_{si}	{@Kd/(@L*@w)}
C_{si}	{@Ke*@L*@w}

The parameterized subcircuit description of the inductor model is in the form:

```
.subckt sp_ind_035 1 2 PARAMS: a1=1.84, a2=0.94,
+ a3=1.36, a4=0.91, b1= -0.76, b2=4.13, b3=0.93, b4= -1.96,
+ beta1=2.5e-4, beta2=6.18e-7, beta3=156, beta4= -4.85e4,
+ c1= -0.14, c2= -1.06, c3= -1.4, c4= -0.83, d1=1.1,
+ d2= -1.9, d4=0.56, e2=1.35, Ka=0.0415e-3, Kb=0.0302,
+ Kc=4.28e-6, Kd=8.04e-6, Ke=2.10e-7, Dout=300u, n=10,
+ sp=5u, w=20u
* the coefficients correspond to the data-fitted monomial
* expressions for CMOS 0.35um process
Rsi2 0 6 {Kd/(4*(Dout-(n*(sp+w)-sp))*n*w)}
Rsub 5 6 {beta3*pwr(n,a3)*pwr((w+sp)*1e6,b3)
+ *pwr(4*(Dout-(n*(sp+w)-sp))*n*1e6,c3)}
Cox2 2 6 {Kc*4*(Dout-(n*(sp+w)-sp))*n*w}
Csi2 0 6 {Ke*4*(Dout-(n*(sp+w)-sp))*n*w}
K1 Ls Lsub {1- exp(beta4*pwr(n,a4)*pwr(Dout*1e6,b4)
+ *pwr(w*1e6,c4)*pwr(sp*1e6,d4))}
Rs 3 2 {Kb*4*(Dout-(n*(sp+w)-sp))*n/w}
Csi1 0 4 {Ke*4*(Dout-(n*(sp+w)-sp))*n*w}
Cox1 1 4 {Kc*4*(Dout-(n*(sp+w)-sp))*n*w}
Cs 1 2 {Ka*n*w*w}
Ls 1 3 {beta1*pwr(Dout*1e6,a1)*pwr(w*1e6,b1)*
+ pwr(sp*1e6,c1)*pwr(n,d1)*1e-9}
Rsi1 4 0 {Kd/(4*(Dout-(n*(sp+w)-sp))*n*w)}
Lsub 4 5 {beta2*pwr(Dout*1e6,a2)*pwr(w*1e6,b2)*
+ pwr(sp*1e6,c2)*pwr(n,d2)*pwr(beta1*pwr(Dout*1e6,a1)*
+ pwr(w*1e6,b1)*pwr(sp*1e6,c1)*pwr(n,d1),e2)*1e-9}
.ends
```

The constants (12) and the independent parameters are defined using the PARAMS statement. The calculation of dependent geometry parameters is included in the expressions for the parameters of the subcircuit elements.

C. Simulation results

The frequency dependencies of the quality factor $Q(f)$, equivalent terminal resistance $ETR(f)$ and the inductance $L(f)$ are obtained using the circuit shown in Fig. 9. The following macrodefinitions in the graphical analyzer *Probe* are defined for the impedance Z_{in} , the quality factor Q and the inductance L of the spiral inductor:

$$\begin{aligned} Z_{in} &= -V(1)/I(V1) \\ R_{in} &= R(Z_{in}) \\ X_{in} &= \text{IMG}(Z_{in}) \\ Q &= X_{in}/R_{in} \\ \pi &= 3.1415965 \\ L &= X_{in}/(2*\pi*\text{frequency}) \end{aligned}$$

The obtained results in *Probe* for $Q(f)$, $ETR(f)$ and $L(f)$ are presented in Fig. 10, Fig. 11 and Fig. 12 correspondingly. The simulation results for $Q(f)$ correspond closely to the measured data $Q_{meas}(f)$ given in [14] (Fig. 10). The maximal relative error for Q does not exceed 5%. This confirms the validity of the developed computer parameterized geometry dependent models. They can be used to adequate modeling of RF circuits, as well as to geometry optimization of spiral inductors using the available optimization tools in CAD programs.

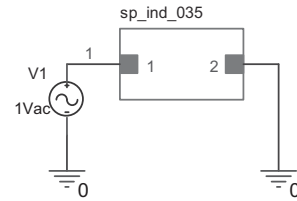


Fig. 9. Circuit for simulation of $Q(f)$ and $L(f)$

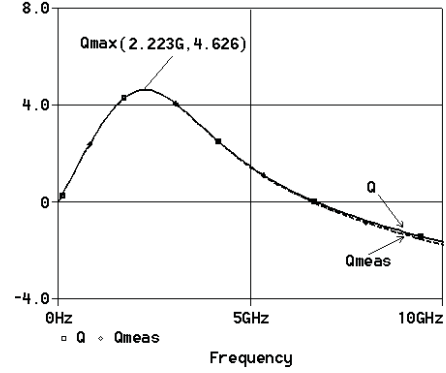


Fig. 10. Simulation results $Q(f)$ and measured data $Q_{meas}(f)$

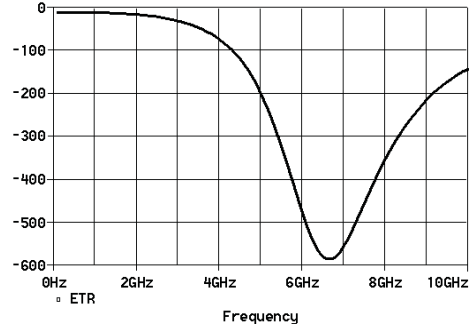


Fig. 11. Simulation results for $ETR(f)$

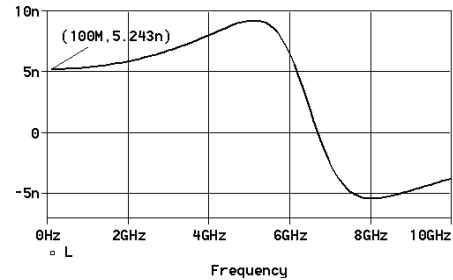


Fig. 12. Simulation results for $L(f)$

IV. CONCLUSIONS

Wide-band geometry dependent SPICE computer models for on-chip planar spiral inductors have been developed using hierarchical blocks. Model descriptions are presented in the form of *PSPice* model and in schematic view. The models are realized in the environment of *Cadence Capture* and *Cadence PSPice*. Model verification is performed demonstrating their validity. The simulation results are in a good agreement with the measurement data. The developed parameterized computer models can be used to adequate computer modeling and simulation of RF circuits, as well as to geometry optimization of planar spiral inductors.

REFERENCES

- [1] C. P. Yue, C. Ryu, J. Lau, T. H. Lee and S. S. Wong, "A physical model for planar spiral inductors on silicon", *Proc. IEEE Int. Electron Devices Meeting Tech. Dig.*, San Francisco, pp. 155-158., CA, Dec. 1996.
- [2] Y.C. Shih, C.K. Pao and T. Itoh,"A broadband parameter extraction technique for the equivalent circuit of planar inductors", *IEEE MTT-S International Microwave Symposium Digest*, pp. 1345-1348, 1992., vol.3, 1-5 Jun 1992.
- [3] J.E. Post,"Optimizing the design of spiral inductors on silicon", *IEEE Trans. on Circuits and Systems - II: Analog and Digital Signal Processing*, pp. 15-17, vol. 47, No 1, Jan. 2000.
- [4] Yu Wenhuan and J.W. Bandler, "Optimization of spiral inductor on silicon using space mapping", *IEEE MTT-S*, pp. 1085-1088, June 2006.
- [5] V. Durev, E. Gadjeva and M. Hristov,"Parameter extraction of geometry dependent RF planar inductor model", *17-th International Conference Mixed Design of Integrated Circuits and Systems -MIXDES'2010*, Wroclaw, June 2010, Poland.
- [6] Y. Cao, R. A. Groves, X. Huang, N. Zamdmer, J. Plouchart, R. Wachnik, T.-J. King and C. Hu, "Frequency-independent equivalent-circuit model for on-chip spiral inductors", *IEEE J. Solid-State Circuits*, vol. 38, no. 3, pp. 419-426, Mar. 2003.
- [7] H. Zou, L. Sun, J. Wen and J. Liu, Scalable modeling and comparison for spiral inductors using enhanced 1-pi and 2-pi topologies, *Journal of Semiconductors*, vol. 31, No. 5, May 2010.
- [8] J. Gil, H. Shin, "A simple wide-band on-chip inductor model for silicon-based RF Ics", *IEEE Transactions on Microwave Theory and Techniques*, vol. 51, n. 9, pp. 2023-2028, Sept., 2003.
- [9] L. Sun, J. Wen, J. Yan, and J. Hu,"Modeling and parameters extraction of spiral inductors for silicon-based RFICs", *Proceedings 7th International Conference on Solid-State and Integrated Circuits Technology*, pp. 224-227, vol. 1,18-21 Oct. 2004.
- [10] J. Wen and L. Sun, "A wide-band equivalent circuit model for CMOS on-chip spiral inductor", *8th International Conference on Solid-State and Integrated Circuit Technology ICSICT '06*, pp. 1383-1385, Shanghai, China, 23-26 Oct. 2006.
- [11] M. Kang, J. Gil and H. Shin,"A simple parameter extraction method of spiral on-chip inductors", *IEEE Transactions on Electron Devices*, pp.1976-1981, vol. 52, n. 9, Sept. 2005.
- [12] H. Chen, H. Zhang, S. Chung, J. Kuo and T. Wu, "Accurate systematic model-parameter extraction for on-chip spiral inductors", *IEEE Transactions on Electron Devices*, pp. 3267-3273, vol. 55, n. 11, Lausanne, Switzerland, Nov. 2008.
- [13] M. Fujishima and J. Kino, "Accurate subcircuit model of an on-chip inductor with a new substrate network," in *Proc. Symp. VLSI Circuits*, Jun. 17-19, 2004, pp. 376-379.
- [14] I. Lai and M. Fujishima, "A new on-chip substrate-coupled inductor model implemented with scalable expressions", *IEEE Journal of Solid-State Circuits*, vol. 41, n. 11, November 2006, pp. 2491-2499.
- [15] *PSpice User's Guide*, Cadence PCB Systems Division, USA, 2000.